PATCH ELECTRODE GLASS COMPOSITION AFFECTS ION CHANNEL CURRENTS

ROY E. FURMAN* AND JACQUELINE C. TANAKA‡
*Departments of *Neurology and ‡Biochemistry and Biophysics, University of Pennsylvania School of Medicine, Philadelphia, Pennsylvania 19104*

ABSTRACT The influence of patch electrode glass composition on macroscopic IV relations in inside-out patches of the cGMP-activated ion channel from rod photoreceptors was examined for a soda lime glass, a Kovar sealing glass, a borosilicate glass, and several soft lead glasses. In several glasses the shape or magnitude of the currents changed as the concentration of EGTA or EDTA was increased from 200 μM to 10 mM. The changes in IV response suggest that, at low concentrations of chelator, divalent cations are released from the electrode glass and interact with the cGMP-activated channel. Possible mechanisms are discussed to explain the observations, and several comments are made concerning the choice of a glass for patching.

INTRODUCTION

Since the discovery of the patch clamp technique (Neher and Sakmann, 1976; Hamill et al., 1981), extensive literature has accumulated about the fabrication and characteristics of patch clamp electrodes. Various investigators have discussed the techniques of pulling and firepolishing the electrodes, the importance of tip geometry, reduction of stray capacitance and slow charge movement, electrical modeling of the gigaseal, electron microscopic studies of the electrode/patch combination, improving the sealing characteristics of cell surfaces, and the selection of glasses to promote gigaseals (Corey and Stevens, 1983; Trube, 1983; Sakmann and Neher, 1983; Rae and Levis, 1984; Jung et al., 1987). Only a few stray cautions have been expressed about the techniques of patch clamping, and little attention has been given to the chemical reactivity of the electrode glass. Recently, however, Cota and Armstrong (1987) described slow inactivation of whole cell potassium currents when patching with 8161 lead potash and soda lime glasses. The inactivation was prevented by high concentrations (10–20 mM) of internal EGTA.

One of our goals is studying selectivity in the cGMP-activated ion channel from rod photoreceptors in the absence of divalent block (Tanaka et al., 1987; Furman and Tanaka, 1987). Difficulties obtaining frequent and reliable gigaseals in the presence of divalent chelators inside and outside the pipette led us to 8161 glass, which markedly enhanced the frequency of patch formation. Although we found aspects of our cGMP-activated current–voltage relations novel, neither the existing photoreceptor literature nor our internal controls initially suggested problems with the data. In light of Cota and Armstrong's abstract (1987), we have examined IV relations in cGMP-activated patches from rod photoreceptors under identical conditions with six electrode glasses. We find that changes in five of the six glasses are affected by increasing the concentration of divalent chelators.

MATERIALS AND METHODS

The retinas of dark adapted frogs (*Rana pipiens*) were dissected under red light and stored in cold frog Ringer's solution (120 mM NaCl, 2.5 mM KCl, 10 mM Hepes, pH 7.4, 1 mM $CaCl_2$, and 1 mM $MgCl_2$) in a light-tight container until needed. Intact rod photoreceptors were harvested by gentle tapping of the container before withdrawing a 10-μl aliquot which was layered onto the floor of the experimental chamber. All experiments were performed in room light at 20°–21°C.

Patch electrodes were fabricated from capillary tubes of N-51A borosilicate (Kimax-51, 1.5–1.8-mm outer diameter [OD], Kimble Products, Toledo, OH), of R-6 soda lime (73811; Kimble Products), of lead potash (8161, 1.65-mm OD, 1.20-mm ID), of two potash soda lead glasses (KG-12 and Corning 0010, 1.60-mm OD, 1.15 ID), or of Kovar 7052 sealing glass (2-mm OD). The latter four glasses were obtained from Garner Glass Co., Claremont, CA. Each glass was from the same lot. The electrodes were pulled in two stages, but not firepolished (except Kovar 7052), to bubble numbers in methanol of 3.0–4.0 and resistances of 8–20 MΩ when filled with standard bath solution (see below).

Electrodes were connected to the headstage of a patch clamp amplifier (model 8900; DAGAN Corp., Minneapolis, MN) by a 120 mM KCl/agar bridge formed from fine polyethylene tubing slipped over the end of an Ag/AgCl wire held in a polystyrene electrode holder (E. H. Wright Co., Guilford, CT). Similar agar bridges were used for ground electrodes and a bath reference amplifier that compensated for the effects of liquid-junction potentials. When measured with respect to a 3 M KCl Ag/AgCl electrode, residual junction potentials were <1 mV. Electrode tip potentials were measured by breaking the pipette tip and also found to be <1 mV. The amplifier output was low pass filtered at 1 kHz (8-pole Bessel, model 902LPF; Frequency Devices, Haverhill, MA) before display on an oscilloscope and digitization by an IBM AT (5 kHz, 12 bit A/D; Labmaster, Scientific Solutions, Solon, OH).

A biphasic voltage ramp was generated by a custom microprocessor-controlled 14-bit D/A converter. Correction for capacitative offset current was done by several techniques: (*a*) maintaining a constant, low solution level with flow; (*b*) electronically compensating residual capacitance; (*c*) digitally combining the up and down ramps; (*d*) employing slow ramps (260 mV/s); and (*e*) digitally computing any residual capacitative current from the leak resistance in symmetrical solutions by comparing the mean holding current at 0 mV before the ramp with the mean current around 0 mV during the ramp (the IV relation is linear in sufficiently small neighborhoods). To speed hardcopy plotting, all current points in the figures represent local 100 μV averages of the digitized response to the voltage ramp at 10 mV intervals.

Inflow to the experimental chamber was via small bore polyethylene tubing attached to a selectable reservoir of twelve solutions. Two banks of six solutions each were manually selected by a Teflon rotary flow valve (type 5011; Rheodyne Inc., Cotati, CA) and the solution from either bank was electronically selected by microvolume two-way Teflon switches at the chamber (P/N LFAA 1201618H; Lee Co., Westbrook, CT). Outflow was via a fine suction capillary covered with a 0.2-μm nylon mesh screen to reduce noise and fluid level fluctuations. After forming an inside-out patch, the pipette tip was positioned in the stream of the inflow tube. Perfusion solutions contacted only plastic syringe barrels, polyethylene, or Teflon.

The standard solution consisted of 120 mM NaCl, 10 mM Hepes-NaOH, pH 7.3, and 200 μM EGTA. When preparing solutions with additional chelators, the total sodium was adjusted to maintain 120 mM. Cells were perfused with standard solution before patching. The pipette and test solutions contained either standard solution or additional EGTA/EDTA as indicated. Photoreceptor currents were activated by 200 μM 3',5'-cGMP added to the test solution.

All currents were measured after digitally subtracting control currents in a solution identical to the test solution, but without cGMP. Currents, potentials, and membrane surfaces are reported in physiological conventions. Experiments comparing voltage ramps with steady-state voltage steps showed no difference in the cGMP-activated channel current nor was any hysteresis evident in the up/down ramps.

RESULTS

The ease with which a particular glass formed a gigaseal to the rod outer segment membrane varied dramatically among the six glasses tested. Kovar 7052 rarely sealed under our conditions (two of 60 attempts). By contrast, 8161 glass would seal spontaneously at the moment of contact with the cell surface despite the presence of a positive pressure applied to the patch pipette. Similar behavior was noted with the other lead-containing glasses, KG-12 and 0010. The R-6 soda lime glass also sealed rapidly, but with relaxation of positive pressure, whereas the N-51A borosilicate glass sealed slowly with the application of negative pressure. Seals ranged from 2 to 10 GΩ for all glasses with no glass consistently forming significantly tighter seals, and the seal resistance was linear for all control currents.

Current–voltage relations were obtained with symmetrical, nominally divalent-free, solutions across an inside-out patch using six different electrode glasses. In 200 μM EGTA, the measured free calcium in the patch solutions was ~0.1 μM. Using identical technique, four distinctly different current–voltage curves were observed with the six glasses (Fig. 1). Two of the lead-based glasses, 8161 and KG-12, consistently, and uniquely, produced a steep inwardly and outwardly rectifying IV relationship (Fig. 1, *A* and *B*). The limiting slopes, however, differed with inward rectification steeper with 8161 glass. Borosilicate, N-51A, and the potash soda lead glass, 0010, produced similar IV's which were slightly concave upward (Fig. 1, *C* and *D*). An outwardly rectifying IV curve qualitatively, but not quantitatively, similar to that recorded under physiological conditions was observed with R-6 (soda lime) glass (Fig. 1 *E*). A concave downward IV was recorded with Kovar 7052 glass (Fig. 1 *F*).

The situation with N-51A and 7052 is actually more complex than apparent in Fig. 1. Fig. 2 illustrates three of the four qualitative types of IV relation described above were obtained with N-51A glass. The source of this variability was not clear, but the steeper outward rectification was more likely at lower current densities (Fig. 2 *A*). The concave downward IV curves with N-51A (Fig. 2 *B*) and 7052 (Fig. 1 *F*), although least frequent, were reversible with cGMP washout and occurred in patches where the leak conductance was less than one-tenth of the cGMP-activated current. The other IV response with 7052 was homologous to the N-51A response in Fig. 1 *C*. This variation in response was not observed with the other glasses despite the same range of current magnitudes and seal resistances. Although the absolute magnitude of patch current occasionally decreased by up to 20% over 10–60 min, changes in IV shape were not seen in a given patch with any glass.

Previous experiments with high concentrations of divalent cations at the intracellular surface of the photoreceptor patch had shown a voltage-independent block of inward monovalent currents (Furman and Tanaka, 1987). To test the possibility that rectification resulted from the effect of a soluble polyvalent metal at the intracellular surface, we titrated the intracellular (bath) side of the patch with increasing concentrations of EGTA while holding extracellular EGTA constant at 200 μM. With 8161 glass the absolute magnitude, but not the shape, of the IV curve increased with titration (Fig. 3). In four experiments, the maximal currents were observed at 7.5–10 mM EGTA. Similar results were obtained with EDTA. Titration of the extracellular surface (inside the pipette) with 200 μM, 1 mM, 5 mM, and 10 mM EGTA steadily changed the shape of the IV curve (Fig. 4, *A* and *B*). In this case, intracellular titration, with 10 mM EGTA extracellularly, did not change the magnitude or shape of the IV curve (not shown). With the other glasses, however, no effect of intracellular titration with EGTA or EDTA was observed at either low or high levels of extracellular chelation.

The effect of high extracellular chelation on the IV response was studied also for R-6, N-51A, and 0010 glasses. With soda lime glass (R-6), 10 mM EGTA inside the pipette (Fig. 4 *C*) had no effect on the shape of the IV curve compared with 200 μM EGTA (Fig. 1 *E*). However, 10 mM EDTA inside the pipette markedly increased the inward sodium current (Fig. 4 *D*) producing an IV curve homologous to that obtained with N-51A (Fig. 1 *C*) and

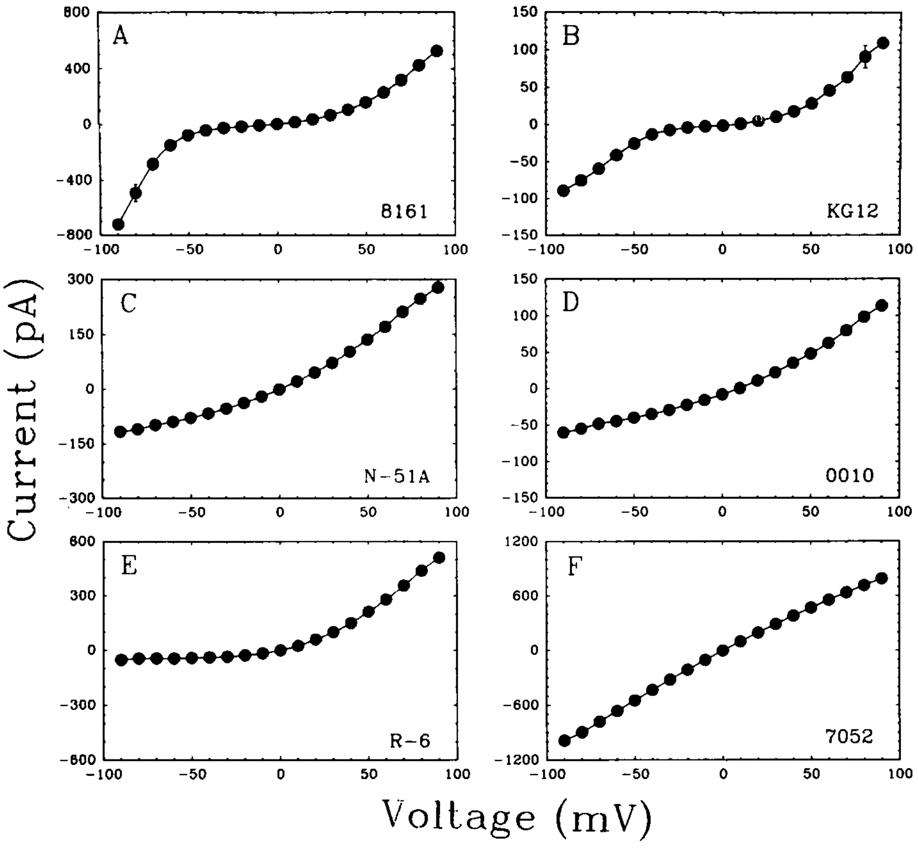

FIGURE 1 Variability of cGMP-activated current–voltage relations in rod photoreceptors observed using different microelectrode glasses. Representative net currents were recorded across inside-out patches using identical protocols and solutions with each glass (see text). (*A*) 8161, lead potash glass response was observed in several hundred patches. (*B*) KG-12, soda lead potash ($n = 2$). (*C*) N-51A, borosilicate. The response shown was seen in 11 of 16 patches. Additional variability with this glass is shown in Fig. 2. (*D*) 0010, soda lead potash glass ($n = 27$). (*E*) R-6, soda lime glass ($n = 6$). (*F*) Kovar 7052, potash glass ($n = 1$ of 2 total, see text). Error bars are standard deviation of the current; most are smaller than the symbols. The range of current magnitudes was similar with all glasses.

0010 (Fig. 1 *D*). Extracellular EDTA and EGTA each produced IV responses in N-51A and 0010 glasses similar to Fig. 1, *C* and *D*, respectively; the variability with N-51A (Fig. 2) was not observed under these conditions.

DISCUSSION

The in situ properties of the cGMP-activated ion channel may explain why this channel is particularly sensitive to the local ionic environment. Under physiological conditions current is carried principally by sodium, but many monovalent species are equally permeable and almost equally conductive (Hodgkin et al., 1985; Yau and Nakatani, 1984). While many divalents also have significant permeability, most are poorly conductive and compete with monovalent ions for passage reducing the apparent channel conductance 1,000-fold (Haynes et al., 1986; Zimmerman and Baylor, 1986). Reduction of single channel current is compensated by a high channel density resulting in a system with a high signal/noise ratio that prevents false triggering from thermal fluctuations. The nonspecificity of polyvalent block and the wide dynamic range of the current result in a high-gain divalent detector. At present,

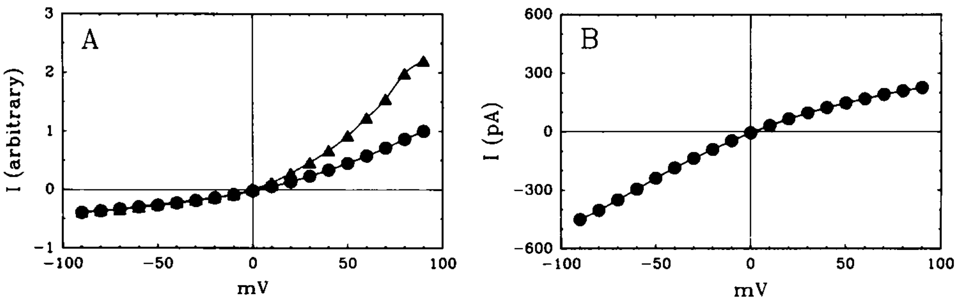

FIGURE 2 Three different IV responses were recorded using borosilicate glass in symmetrical 120 mM Na, 200 uM EGTA standard solution. (*A*) Responses from two patches were arbitrarily scaled to emphasize the differences in shape. The peak outward current (632 pA) of the most common IV response (11 of 16 patches) was normalized to 1 (●). The next most common response (3 of 16 patches) was scaled by 0.034 to maximize congruence of the inward currents (original peak outward current was 66 pA). The lower curve (●) is congruent with the 0010 glass response (Fig. 1 *D*) whereas the upper curve (▲) is congruent with the soda lime response (Fig. 1 *E*). (*B*) The concave downward response was obtained in 2 of 16 patches with borosilicate, and in 1 of 2 Kovar 7052 patches (Fig. 1 *F*). IV response variability with a single glass was not seen with soda lime or any of the lead-based glasses.

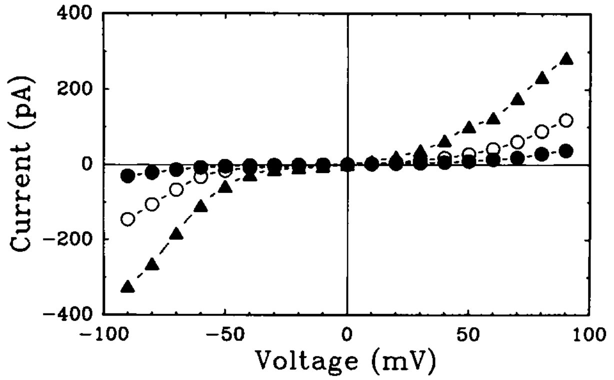

FIGURE 3 Intracellular titration of an inside-out patch formed across an 8161 glass pipette by EGTA. The patch was formed in standard symmetrical solution (120 mM Na, 200 μM EGTA), and successively higher concentrations of EGTA (200 μM; 1, 2, 5, 7.5, 10 mM) in 120 mM total Na were perfused through the chamber. The leak current at each EGTA concentration in the absence of cGMP was subtracted from the total current activated by 200 μM cGMP. (●) 2 mM EGTA; (○) 7.5 mM EGTA; (▲) 10 mM EGTA. Current magnitudes from 200 μM to 2 mM were identical. All curves were congruent when linearly scaled.

however, the biophysical details of ion selectivity, channel gating, and ligand activation are insufficiently characterized to predict the ions and mechanism generating the specific IV curves recorded with each microelectrode glass.

The effects of glass composition on the cGMP-activated ion channel in patches and on the K^+ channel from cultured pituitary cells (Cota and Armstrong, 1987) may be most simply interpreted as channel block by a soluble polyvalent cation as evidenced by the titratable chelator effects and known divalent blocking effects. Alternative explanations, such as glass–membrane interfacial forces differentially stressing the patched membrane and secondarily influencing channel function, are possible for patch data, but seem less plausible explaining Cota and Armstrong's observations with whole cell macroscopic currents.

Important for understanding, and avoiding, the "biological effects of glass" are knowing the species of interfering ion(s), the free concentration, and the mechanism producing the soluble species. To these questions our data and the glass technology literature only suggest possibilities.

The R-6 (soda lime) IV (Fig. 1 *E*) resembles the in situ photoreceptor IV in which Ca^{2+} is thought to produce a voltage-relieved, extracellular block of the channel (Baylor and Nunn, 1986). The striking relief of block by extracellular EDTA, but not by EGTA (Fig. 4, *C* and *D*), however, suggests Mg^{2+} is the (co-)blocking cation in R-6. Inspection of the composition of R-6 glass (Table I) shows both Mg^{2+} and Ca^{2+} are present in molar concentrations.

The high lead concentration in 8161 and KG-12 glasses (Table I) makes Pb^{2+} suspect as the blocking species, but several circumstantial arguments suggest this may not be the case. First, addition of 10 μM extracellular Pb^{2+} with N-51A electrodes did not produce the characteristic IV relation, but rather generated the infrequent IV relation similar to Fig. 1 *F*. Second, only one of the two potash soda lead glasses demonstrated block despite similar lead contents (4 and 3 M). Third, if Pb^{2+} is the blocking ion in 8161

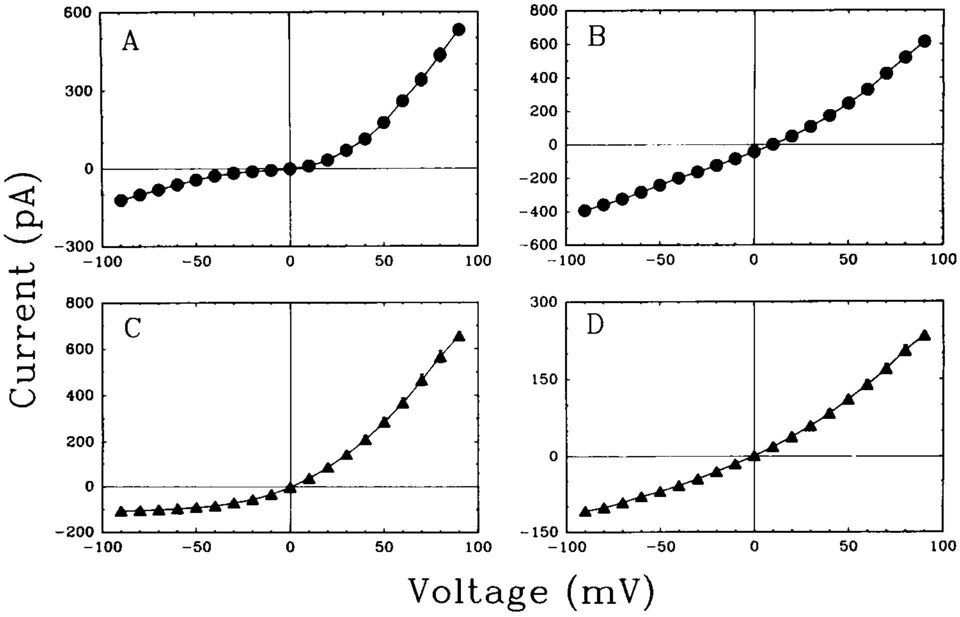

FIGURE 4 Extracellular chelation of divalent cations in 8161 glass (*A*, *B*) and in R-6 glass (*C*, *D*). A series of inside-out patches were formed with the symmetrical chelator concentrations across the patch. IV curves obtained with 8161 glass showed modest shape changes at 1 mM (not shown) and 5 mM EGTA (*A*) compared with 200 μM EGTA (Fig. 1 *A*), but 10 mM EGTA (*B*) eliminated the characteristic biphasic rectification. Similar currents were recorded with 10 mM EDTA extracellularly (not shown). Three consecutive IV curves with soda lime glass in 10 mM EGTA (*C*) showed no difference compared with 200 μM EGTA (Fig. 1 *E*), but 10 mM EDTA (*D*) decreased the ratio of outward/inward current ($n = 3$).

TABLE I

COMPOSITION OF ELECTRODE GLASS (MOLAR)

	R-6	N-51A	8161	KG-12	0010	7052
SiO_2	28.0	28.4	26.0	28.7	31.0	30.7
B_2O_3	0.6	4.0				8.9
Al_2O_3	0.7	1.7	0.08	0.5		2.1
PbO	<0.002	<0.002	9.2	4.0	3.0	<0.003
BaO	0.3	0.3	0.5			0.5
CaO	2.6	0.4	0.2	0.05	0.2	0.1
MgO	2.5	0.03	0.04	0.08	0.08	0.07
Na_2O	6.2	2.5	0.1	1.8	3.5	1.1
K_2O	0.2	0.2	2.9	2.8	2.4	0.9
As_2O_3		<0.002	0.02		0.06	
SO_3	0.06					
Li_2O						0.6
Sb_2O_3			0.05		0.03	
Softening temp. (°C)	700	798	604	632	625	716
Density	2.47	2.36	4.0	3.05	3.05	2.84

and KG-12 glasses, the solubility product of $PbCl_2$ in our solutions constrains the free [PB^{2+}] to ~700 μM. However, as both EGTA and EDTA stability constants for Pb^{2+} are at least four and seven orders of magnitude greater than those for Ca^{2+} or Mg^{2+} (Martell and Smith, 1974), and at least 5 mM chelator was required to see a substantial change in current, the unchelated equilibrium free [Pb^{2+}] must be >700 μM. Finally, while the crystal structure of silica lead glasses is not known with certainty, lead forms asymmetric coordinate bonds with four neighboring oxygens and is unlikely to participate significantly in surface reactions with the aqueous phase (Kreidl, 1983).

Other potential interfering ions common to 8161 and KG-12 glasses include Al^{3+}, Ca^{2+}, and Mg^{2+}. Surface exchange of Al^{3+} is energetically unfavorable as it also forms coordinate bonds with bridging oxygens. The alkaline earth oxides, on the other hand, charge compensate pairs of non-bridging oxygen atoms in the silica glass network and would be more readily exchangeable with cations in solution. The identical changes in IV characteristics with both EGTA and EDTA at similar concentrations probably excludes Mg^{2+} leaving Ca^{2+} as the suspect. But why would Ca^{2+}, which is common to all glasses examined, be soluble only in certain glasses? The molecular structure, physical properties, and solid-liquid phase equilibria of mixed alkali silicate glasses is incompletely understood, but it is known that specific physical properties exhibit maxima or minima as a function of the mole fraction composition of the glass (Kreidl, 1983; Baucke, 1985). By the same argument, barium or the fining agents, arsenic and antimony, may be the reactive species in 8161 glass.

The concentrations of soluble blocking species are substantial with R-6 and 8161 as attested by the 5–10 mM of chelator required to eliminate the blocking effect both in our patches and in Cota and Armstrong's whole cell preparations. Although the $K_{1/2}$ for extracellular Mg^{2+} and Ca^{2+} block in the cGMP-activated channel is unknown, a reasonable estimate is 10–100 μM (Zimmerman and Baylor, 1987). Under this assumption, the end point of free metal titration determined by noting the rapid changes in membrane current with small increases of chelator would overestimate free metal concentration, at most, by 1.5–3× only if the apparent stability constant of the metal-chelator were of the same order of magnitude as the metal-channel affinity constant (Reilley and Schmid, 1959). Of all the possible blocking species in Table I, only Mg^{2+} and Ba^{2+} have sufficiently small apparent stability constants for this to occur (Martell and Smith, 1974).

The origin of the variability in IV curves seen with N-51A is unlikely to be biological as it was not seen with the other glasses despite similar current ranges. If soluble ionic species are responsible for the variability of N-51A glass, then the pipette surface area/solution volume ratio in the vicinity of the patch and a significantly lower concentration of exchangeable species at the glass surface may be the causes since we observed that patches with smaller currents showed greater deviation from linearity.

Soluble ions are produced from oxide glasses by complex interactions between equilibrium surface responses at the glass–solution interface and non-equilibrium interdiffusion processes between the bulk glass and the interfacial glass layer (Baucke, 1985). At the glass–solution interface, multiple equilibria exist including pH-dependent dissociation of silanol groups and enthalpy driven metal siloxy dissociations and exchanges for each cationic species in the glass and solution. The resulting changes in surface concentrations of the reactive species drive concentration-dependent interdiffusions between the bulk glass and interfacial layer. In addition, the silicon network of the glass interfacial layer is undergoing catalytic hydrolysis by aqueous H^+ or OH^- ions. The overall processes in the glass of interfacial formation and network dissolution are thermodynamically unstable creating a net metal loss to, or a net cation exchange with, the solution at a rate advancing with the square root of time (diffusion-limited). The ionic mobilities within the glass and the rates of network hydrolysis are sufficiently slow that they do not disturb the surface equilibria, but they retard formation of a steady state for hours or days. The surface equilibria respond rapidly to changes in aqueous ionic activities as described by Eisenman's general equation for glass electrodes (Eisenman, 1962), but the non-equilibrium interdiffusion processes source or sink aqueous metal cations at a steady rate during the typical time-course of patch clamping. The quantity of metal generated depends on concentrations of species in the glass as well as multiple, interdependent reaction rates, and is not easily predictable by knowing the glass composition.

Solubilization of alkali vapors condensed onto the glass surface during manufacture (or firepolishing) may also account for the interfering ions. Studies of free alkali extractable with cold water rinses after manufacture of commercial glass bottles found an inverse relationship between the amount of extracted alkali and the area of the bottle opening (Budd and Kirwan, 1962). The outer surface of the bottle was alkali free. Warming the bottles to 50°C in a humid atmosphere before capping them increased the extractable alkali as did storage. The study concluded that alkali vaporized at elevated surface temperatures during bottle formation, but the partially enclosed volume limited escape causing alkali to recondense onto the interior glass surface during cooling. In the soda lime glass studied, extractable alkali ranged from 2 to 300 μg Na_2O/dm^2 glass surface. In a micropipette, the concentrations might range as high as 4 mM at the tip to 1.5 μM in the barrel.

The question whether any of the glasses examined are physiological inert is moot. The slightly concave upward curves common to N-51A (Fig. 1 *C*), 0010 (Fig. 1 *D*), and both 8161 (Fig. 4 *B*) and R-6 (Fig. 4 *D*) after chelation are all congruent, suggesting that this is the true macroscopic IV relation. Of the six glasses examined, only 0010 consistently produced this IV relation at all chelator concentrations. The variability of response found with N-51A glass, however, emphasizes more stringent criteria may be required, such as single channel analysis of kinetic and conduction behavior, before accepting a candidate glass as inert.

CONCLUSIONS

We feel the observations of Cota and Armstrong and our data warrant the following conclusions and cautionary notes: (*a*) No patch electrode glass can be considered a priori physiologically inert. Each glass and biological system must be individually tested for interfering effects. (*b*) Divalent and probably monovalent species can exist at high local concentrations requiring 5–10 mM chelator concentrations before their effects are no longer observed. (*c*) Ion effects at both the bath and inside surfaces of the pipette must be considered. (*d*) A family of glasses sharing similar composition must not be judged fit or unfit for patch clamping by the performance of one or more members. (*e*) The presence or absence of physiological effects may be subtle and depend on the local geometry the patch and electrode. (*f*) Patch electrode pulling and firepolishing may contribute to soluble ions if the alkali evaporation–recondensation mechanism in a restricted space is quantitatively significant.

We thank Paul Mueller for his advice and support.

This work was supported by grants NS00865, University Research Fund, and BRSG S07-RR-05415-26 to R. E. Furman, EY06640 to J. C. Tanaka, and GM25256 to P. Mueller.

Received for publication 16 June 1987 and in final form 19 October 1987.

REFERENCES

Budd, S. M., and J. J. Kirwan. 1962. Alkali mobility at glass surfaces during forming and annealing, and its effect on the chemical properties of the surface. *In* Advances in Glass Technology. American Ceramic Society, editor. Plenum Publishing Corp., New York. 527–540.

Baucke, F. G. K. 1985. The origin of the glass electrode response. *In* Glass. Current Issues. A. F. Wright and J. Dupuy, editors. Marinus Nijhoff Publishers, Dordrecht. 481–505.

Baylor, D. A., and B. J. Nunn. 1986. Electrical properties of the light-sensitive conductance of salamander rods. *J. Physiol. (Lond.)*. 371:115–145.

Corey, D. P., and C. F. Stevens. 1983. Science and technology of patch-recording electrodes. *In* Single-Channel Recording. B. Sakmann and E. Neher, editors. Plenum Publishing Corp., New York. 53–68.

Cota, G., and C. M. Armstrong. 1987. Whole-cell recorded K currents using the patch-clamp technique are influenced by the glass of the patch pipette. *Biophys. J.* 51:49a. (Abstr.)

Eisenman, G. 1962. Cation selective glass electrodes and their mode of operation. *Biophys. J.* 2:259–323.

Furman, R. E., and J. C. Tanaka. 1987. Ion selectivity of the cGMP-activated conductance from photoreceptors. *Biophys. J.* 51:17a. (Abstr.)

Hamill, O. P., M. E. Neher, B. Sakmann, and F. J. Sigworth. 1981. Improved patch-clamp techniques for high-resolution current recording from cells and cell-free membrane patches. *Pfluegers Arch. Eur. J. Physiol.* 391:85–100.

Haynes, L. W., A. R. Kay, and K.-W. Yau. 1986. Single cyclic GMP-activated channel activity in excised patches of rod outer segment membrane. *Nature (Lond.)*. 321:66–70.

Hodgkin, A. L., P. A. NcNaughton, and B. J. Nunn. 1985. The ionic selectivity and calcium dependence of the light-sensitive pathway in toad rods. *J. Physiol. (Lond.)*. 358:447–468.

Jung, F., M. J. Song, and F. Sachs. 1987. Patch clamp anatomy: high voltage electron microscopy of in vivo patches. *Biophys. J.* 51:517a. (Abstr.)

Kreidl, N. J. 1983. Inorganic glass-forming systems. *In* Glass: Science and Technology. D. R. Uhlmann and N. J. Kreidl, editors. Academic Press, Inc., New York. 105–299.

Martell, A. E., and R. M. Smith. 1974. Critical Stability Constants. Vol. 1. Amino Acids. Plenum Publishing Corp., New York.

Neher, E., and B. Sakmann. 1976. Single channel currents recorded from membrane of denervated frog muscle fibers. *Nature (Lond.)*. 260:799–802.

Rae, J. L. and R. A. Levis. 1984. Patch voltage clamp of lens epithelial cells: theory and practice. *Mol. Physiol.* 6:115–162.

Reilley, C. N., and R. W. Schmid. 1959. Principles of end point detection in chelometric titrations using metalochromic indicators: characterization of end point sharpness. *Anal. Chem.* 31:887–897.

Sakmann, B., and E. Neher. 1983. Geometric parameters of pipettes and membrane patches. *In* Single-Channel Recording. B. Sakmann and E. Neher, editors. Plenum Publishing Corp., New York. 37–51.

Tanaka, J. C., R. E. Furman, W. H. Cobbs, and P. Mueller. 1987. Incorporation of a retinal rod cGMP-dependent conductance into planar bilayers. *Proc. Natl. Acad. Sci. USA*. 84:724–728.

Trube, G. 1983. Enzymatic dispersion of heart and other tissues. *In* Single-Channel Recording. B. Sakmann and E. Neher, editors. Plenum Publishing Corp., New York. 69–76.

Yau, K.-W., and K. Nakatani. 1984. Cation selectivity of light-sensitive conductance in retinal rods. *Nature (Lond.)*. 309:352–354.

Zimmerman, A. L., and D. A. Baylor. 1986. Cyclic GMP-sensitive conductance of retinal rods consists of aqueous pores. *Nature (Lond.)*. 321:70–72.